Journal of Radiation Research, 2015, 56, 269–277
doi: 10.1093/jrr/rru098 Advance Access Publication 24 November 2014

Radiation response of mesenchymal stem cells derived from bone marrow and human pluripotent stem cells

Mohammad S. ISLAM[1], Melissa E. STEMIG[1], Yutaka TAKAHASHI[2] and Susanta K. HUI[2,3,*]

[1]School of Dentistry, University of Minnesota, 420 Delaware Street SE, Mayo Mail Code 494, Minneapolis, MN 55455, USA
[2]Masonic Cancer Center, University of Minnesota, 420 Delaware Street SE, Mayo Mail Code 494, Minneapolis, MN 55455, USA
[3]Department of Therapeutic Radiology, University of Minnesota, 420 Delaware Street SE, Mayo Mail Code 494, Minneapolis, MN 55455, USA
*Corresponding author. Department of Therapeutic Radiology, University of Minnesota, 420 Delaware Street SE, Mayo Mail Code 494, Minneapolis, MN 55455, USA. Tel: +1-612-626-4484; Fax: +1-612-626-7060; Email: huixx019@umn.edu

(Received 9 April 2014; revised 30 August 2014; accepted 29 September 2014)

Mesenchymal stem cells (MSCs) isolated from human pluripotent stem cells are comparable with bone marrow-derived MSCs in their function and immunophenotype. The purpose of this exploratory study was comparative evaluation of the radiation responses of mesenchymal stem cells derived from bone marrow- (BMMSCs) and from human embryonic stem cells (hESMSCs). BMMSCs and hESMSCs were irradiated at 0 Gy (control) to 16 Gy using a linear accelerator commonly used for cancer treatment. Cells were harvested immediately after irradiation, and at 1 and 5 days after irradiation. Cell cycle analysis, colony forming ability (CFU-F), differentiation ability, and expression of osteogenic-specific runt-related transcription factor 2 (RUNX2), adipogenic peroxisome proliferator-activated receptor gamma (PPARγ), oxidative stress-specific dismutase-1 (SOD1) and Glutathione peroxidase (GPX1) were analyzed. Irradiation arrested cell cycle progression in BMMSCs and hESMSCs. Colony formation ability of irradiated MSCs decreased in a dose-dependent manner. Irradiated hESMSCs showed higher adipogenic differentiation compared with BMMSCs, together with an increase in the adipogenic PPARγ expression. PPARγ expression was upregulated as early as 4 h after irradiation, along with the expression of SOD1. More than 70% downregulation was found in Wnt3A, Wnt4, Wnt 7A, Wnt10A and Wnt11 in BMMSCs, but not in hESMSCs. hESMSCs are highly proliferative but radiosensitive compared with BMMSCs. Increased PPARγ expression relative to RUNX2 and downregulation of Wnt ligands in irradiated MSCs suggest Wnt mediated the fate determination of irradiated MSCs.

Keywords: mesenchymal stem cell; human pluripotent stem cell; radiation effect; osteogenesis; adipogenesis

INTRODUCTION

Hematopoietic malignancies are often treated with radiation therapy as a conditioning regimen prior to bone marrow transplant, and further increase in focused radiation to bone marrow is under way to enhance its therapeutic advantage for leukemia [1, 2]. However, little is known about how radiation might damage bone marrow stromal/stem cells (MSCs), an essential component of the bone marrow microenvironment. Radiation-induced damage to marrow cells in particular is important, as this leads to osteoporosis, fracture and poor healing. Radiation used to kill solid tumors also causes acute myelosuppression, residual marrow injury, loss of hematopoietic stem cells (HSCs), and damage to MSCs [3–5]. Such adverse effects can be irreversible and fatal. Thus, potential treatment options must minimize the adverse effects on hematopoiesis and bone cells, while eliminating the cancer cells from marrow. This goal has been partially achieved by transplanting bone marrow stromal/stem cells (MSCs), which contain stem cells of hematopoietic and mesenchymal lineage. In animal models, infusion of MSCs successfully reconstituted hematopoiesis that had been lost due to radiation [6]. Therefore, understanding the functional and morphological response of MSCs to radiation exposure may

elucidate the mechanisms underlying the recently observed bi-directional co-regulation of bone and marrow components at the micro-environmental level [7, 8].

MSCs are heterogeneous cells that include the progenitor cells for osteoblasts, chondrocytes and adipocytes. MSCs have been described as supportive cells for marrow hematopoiesis. MSCs, like hematopoietic cells, are sensitive to radiation, but to a lesser extent. This relative radiation resistance of MSCs is likely to be one of the important contributing factors for their ability to rescue hematopoiesis after radiation damage. MSCs are found in multiple tissues, including muscle, blood vessels, the central nervous system and dental pulp. More recently, MSCs have been derived from human embryonic stem cells (hESMSCs) and induced pluripotent stem cells (iPSCs) [9]. Specifically, pluripotent stem cell technology has made it possible to use somatic cells from a patient to develop MSCs [10, 11], which would carry lower risk of rejection when used for transplant. Moreover, bone marrow-derived MSCs (BMMSCs) show reduced differential potential and lower therapeutic efficacy when expanded several times [12]. This limits repeated use of BMMSCs for experimental and therapeutic needs.

Recently, Nicolay *et al.* characterized bone marrow-derived MSCs after irradiation in comparison with human primary fibroblasts [13]. However, it is unknown whether hESMSCs carry a similar therapeutic potential to that of BMMSCs in patients receiving ionizing radiation. As the first step toward making this determination, irradiated hESMSCs and BMMSCs were compared for genetic and functional properties. Here we demonstrate that irradiated MSCs from these two sources have distinctly different responses to ionizing radiation.

MATERIALS AND METHODS

Mesenchymal stem cell isolation

Bone marrow stromal cells were obtained from a commercial source (Lonza, Walkersville, MD). The human embryonic stem cell (hESC) line WA09 (Wicell Institute, Madison, WI) was used for derivation of MSCs. hESCs were cultured on 80-Gy γ-irradiated mouse embryonic fibroblasts (MEF, Chemicon, Millipore, Billerica, MA) [14]. MSCs were developed using the previously described protocol [15]. Briefly, undifferentiated hESCs were co-cultured with mitomycin C-treated (Bedford Laboratories, Bedford, OH) mouse bone marrow-derived cells (M210, ATCC, Manassas, VA) in the presence of 15% fetal bovine serum (FBS) for three weeks. The presence of serum induces the formation of the three germ layers and the further development of progenitor cells including mesenchymal stem cell-like cells [16]. The cells were then harvested and sorted for MSC-specific CD34 and CD73 (BD BioSciences, Franklin Lakes, NJ) dual expression using magnetic nanoparticles in the EasySep Selection Kit (Stem Cell Technologies, Vancouver, BC, Canada). These $CD73^+/CD34^+$ cells (hESMSCs) were used as MSCs to study radiation-induced changes. The MSC-like phenotype of hESMSC was also verified using CD90, CD105 and CD146 (See Supplementary Table S1).

Irradiation of cells

When BMMSCs and hESMSCs reached 80% confluency, they were irradiated with 2, 4, 8 and 16 Gy by 6-MV X-ray beams from a linear accelerator in clinical use (Varian Medical Systems, Palo Alto, CA). Control groups of cells were placed in the linear accelerator but not exposed to irradiation. Culture vessels were irradiated in the field size of 20×20 cm^2 with the Source-to-Surface-Distance of 100 cm on the 1.5-cm bolus. The dose rate was 400 cGy/min. The dose output was calibrated daily to keep the consistency of the radiation dose to within 2%. Furthermore, the dose at the plane beneath the cells was verified by a GafChromic EBT-3 film (ISP Technologies Inc., Wayne, NJ), confirming that it was within 5% of the planned dose. The culture media (α-MEM, Gibco/Invitrogen, Grand Island, NY), supplemented with 10% FBS, was replaced immediately after irradiation.

RNA isolation, cDNA synthesis and gene expression

Total RNA was harvested from BMMSCs and hESMSCs with or without irradiation using Qiashredder and RNeasy Micro kits (Qiagen, Valencia, CA) according to the manufacturer's protocols. The RNA was then used to synthesize complementary DNA (cDNA) using SuperScript III reverse transcriptase (200 U of RT, 0.5 mM dNTP, 40 U of RNAse OUT, 5 mM DTT, and oligo dT 12–18 bp; Invitrogen). The cDNA was then amplified and run on a 1.5% TAE-ethidium bromide agarose gel to confirm viability of the synthesized cDNA. Non-irradiated and irradiated MSCs were quantified for relative expression of osteogenic-specific runt-related transcription factor 2 (RUNX2), adipogenic peroxisome proliferator-activated receptor gamma (PPARγ), oxidative stress specific superoxide dismutase 1 (SOD1) and glutathione peroxidase 1 (GPX1). Quantitation of gene expression relative to glycerol 3-phosphate dehydrogenase (GPDH) was determined using a Stratagene Thermocycler (La Jolla, CA) and the delta delta CT (ddCT) method [17].

For gene expression array, cDNA was synthesized according to the manufacturer's instructions included in the array (SABiosciences, Catalogue #330401). cDNA was used to study the human Wnt signaling pathway (SABiosciences, Catalogue #PA HS-043ZA). The array was repeated using cDNA from control and irradiated BMMSCs and hESMSCs (2 Gy) from two or three separate experiments. The results were analyzed using the SABiosciences web analysis tool.

Cell cycle

The cell cycle distributions in BMMSCs and hESMSCs were studied by flow cytometric analysis of propidium iodide (PI)-stained cells. The cells with or without irradiation were

trypsinized and harvested 1 day and 5 days after irradiation and fixed with 75% ethanol at a concentration of 1×10^6 cells/ml. The cells were then stained with 20 μg/ml propidium iodide, 500 μg/ml RNAse A (both from Sigma Aldrich, St Louis, MO), 1% Triton X-100 (Thermo Fisher Scientific, Waltham, MA), incubated at 37°C in the dark for 30 min then analyzed on a FACScan flow cytometer (BD Biosciences, Franklin Lakes, NJ). The cell populations were gated as judged by side scatter versus forward scatter, and the percentage of cells in various stages of the cell cycle was calculated using Cyflogic software (CyFlo Ltd, Turku, Finland).

To study MSC-specific surface markers (CD73, CD90, CD105 and CD146, all from BD Biosciences), cells were harvested and stained with antihuman antibodies specific for these cell surface molecules. The cells were incubated with the specific antibodies for at least 20 min at 4°C in the dark, washed in phosphate-buffered saline (PBS, Gibco/Invitrogen) once and resuspended in PBS containing 1% FBS. Flow analysis was performed using a FACScan flow cytometer.

CFU-F assay

Cells were plated at a density of 1000 cells in a T25 (25 cm^2) flask and incubated in a 37°C incubator under a 5% CO_2 atmosphere. The media was replaced every 3 days. At Day 14, cells were fixed with methanol and stained with Giemsa stain (Sigma-Aldrich, St Louis, MO). Colonies containing at least 30 cells were counted. The average colony numbers of three independent experiments were obtained.

Osteogenic and adipogenic differentiation of irradiated MSCs

BMMSCs and hESMSCs were irradiated in T25 flasks and immediately plated with osteogenic or adipogenic medium to induce osteogenic and adipogenic differentiation. Specifically, osteogenesis was induced in the presence of ascorbic acid (0.1 M), dexamethasone (10^{-4} M) and β-glycerol phosphate (500 mM) [15]. Differentiated cells were stained on Day 21 or 28 for osteogenic mineralization using Von Kossa staining. Adipogenesis was induced in the presence of insulin (2 mg/ml), isobutyl methyl xanthine (IBMX, 100 mM), indomethacin (10 mg/ml) and dexamethasone (10^{-3} M) in MSC basal media [15]. Adipogenic cells were stained after Day 21 using Oil Red O (Millipore, Billerica, MA).

Statistical analysis

The statistical significance of the results for different types of MSCs and different dose levels were analyzed using analysis of variance (ANOVA). Multiple comparisons between groups were made with the Tukey–Kramer adjustment for *P*-values and confidence limits. Two-tailed independent *t* tests were conducted to examine whether the responses to irradiation were significantly different between BMMSCs and hESMSCs. Statistical analyses were performed using Dr. SPSS II software (IBM, New York, NY) and a two-tailed *P*-value of <0.05 was considered statistically significant.

RESULTS

Irradiation alters cell cycle progression

After one day of radiation, the percentages of cells in S phase decreased in both types of MSCs (Fig. 1). This was accompanied by a dose-dependent increase in the cell percentage in either G1 or G2/M phase. BMMSCs accumulated in the G1 phase, suggesting an inhibition of the progression of cells from G1 to S phase and a stop in the G1 to S transition. hESMSCs on the other hand accumulated in the G2/M phase, indicating a G2 arrest. The differences in cell cycle distribution between BMMSCs and hESMSCs were statistically significant, as shown in Fig. 1c. Thus, irradiation differentially halted the cell cycle of BMMSCs and hESMSCs (G1 vs G2/M) 1 day after radiation. There were no differences in the cell cycle distribution in G1, S or G2/M transition phases between irradiated and non-irradiated control cells 5 days after irradiation (See Supplementary Fig. S1).

Effects of radiation on colony formation by MSCs

There were fewer colonies formed by both types of irradiated MSCs at 14 days after radiation when compared with the non-irradiated group (Fig. 2a). Non-irradiated hESMSCs showed significantly higher proliferation (i.e. number of colonies formed) compared with BMMSCs ($P = 0.007$) (Fig. 2b). Colony-forming ability decreased in both types of MSCs in a dose-dependent manner. Notably, at 16 Gy, no colony containing >30 cells was formed. Morphologically consistent with senescent MSCs [18], the cells were enlarged, yet fibroblastic and attached to the culture dish at 14 days after radiation with 16 Gy.

Radiation effects on differentiation ability of MSCs

Von Kossa staining showed decreased staining for mineralized nodules formed by BMMSCs and hESMSCs irradiated with 4 Gy (Fig. 3a). This decrease was noted in a dose-dependent manner. Irradiation of 16 Gy did not form colonies as shown in Fig. 2, thus no mineralized nodules were formed. Adipogenic differentiation was detected after 21 days of differentiation. hESMSCs showed higher adipogenic differentiation at 4 Gy compared with BMMSCs (Fig. 3b).

One of the complications of radiation therapy is marrow adipogenesis, with a concomitant loss of osteogenesis. We therefore analyzed the ratio of adipogenic PPARγ to osteogenic RUNX2 expression in the irradiated and non-irradiated controls (Fig. 4a). The ratio of PPARγ to RUNX2 was elevated in both types of MSCs 1 day after irradiation of 2 Gy. In the hESMSCs only, this was further increased at 4 Gy and dropped at 16 Gy. At 5 days after radiation, the ratio of PPARγ to RUNX2 had not changed in hESMSCs, whereas in BMMSCs, the ratio had increased with 2 Gy and 4 Gy

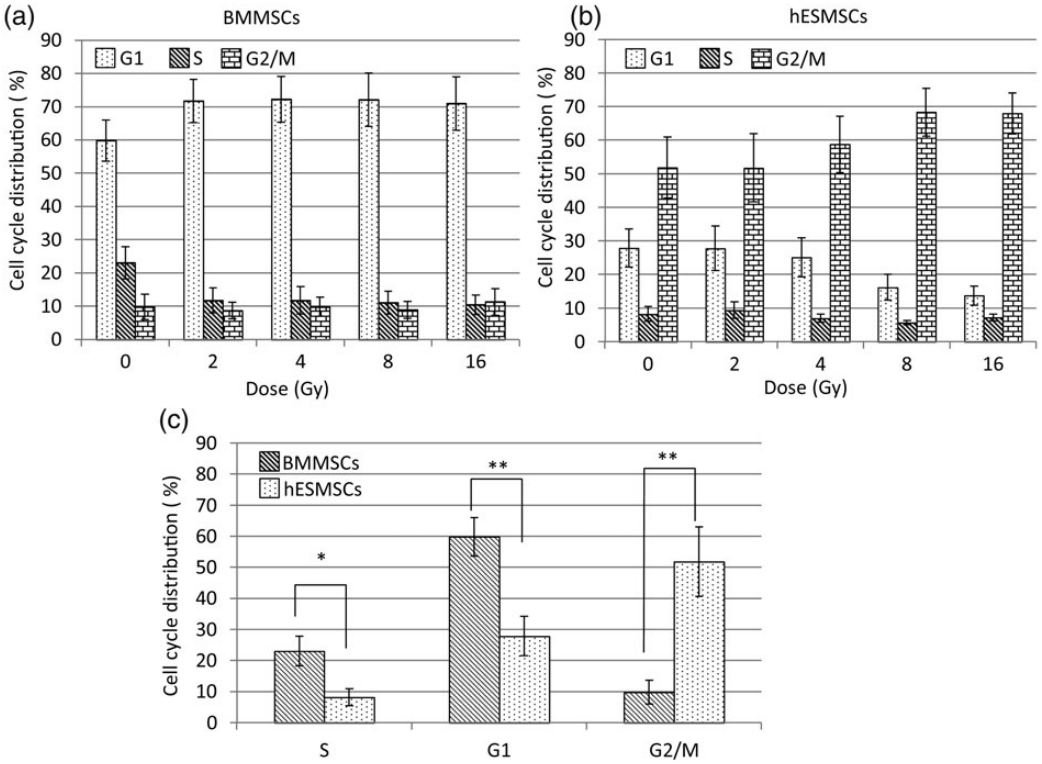

Fig. 1. Cell cycle distributions in (**a**) BMMSCs ($n = 6–7$), and (**b**) hESMSCs ($n = 4–5$) 1 day after irradiation or without irradiation. (**c**) The difference in cell cycle distribution between BMMSCs and hESMSCs. The majority of BMMSCs were in G1 phase, whereas the majority of hESMSCs were in G2/M phase. Percentage of cells in those phases increased in a dose-dependent manner. Statistically significant differences were observed between BMMSCs and hESMSCs. Bars represent mean and standard error: $*P < 0.05$; $**P < 0.01$.

doses and dropped with 16 Gy. These trends were not statistically significant.

Differential expression of oxidative stress and lineage-specific genes in irradiated cells

SOD1 expression increased in both types of MSCs 1 day after radiation (Fig. 4b). hESMSCs demonstrated higher expression of SOD1 for all the radiation doses compared with BMMSCs. The highest increase in SOD1 expression was observed with 2 Gy irradiation, indicating initiation of a cell response even at a low dose. Expression of GPX1 was only slightly increased (Fig. 4c). This pattern was less obvious at Day 5 after irradiation for both types of MSCs.

Radiation inhibits expression of Wnt ligands

Activation of the Wnt pathway has been shown to suppress adipogenic PPARγ expression [19]. In order to understand how radiation affects the Wnt pathway, expression of Wnt ligands was studied using a human Wnt signaling array from SA Biosciences. The array includes 83 Wnt-related genes, including 16 Wnt ligands. These ligands are secreted proteins that bind to cell surface receptors to stimulate the signaling cascade. Figures 5a and b show heatmaps of fold up- or downregulations of Wnt-related genes (illustrated in Fig. 5c). We found expression of five Wnt ligands (Wnt3A, Wnt4, Wnt7A, Wnt10A and Wnt11) was ≥70% downregulated in BMMSCs 4 h after 2 Gy irradiation compared with non-irradiated controls (Fig. 5d). Wnt6 was also downregulated by 65%. On the other hand, different set of ligands (including beta-catenin) were downregulated in the irradiated hESMSCs. The results of the PCR array analysis can be accessed in the National Center for Biotechnology Information Gene Expression Omnibus database (Reference number: GSE60310).

DISCUSSION

In the present study, we determined radiation-induced changes in the colony-forming ability, cell cycle progression, differentiation ability and gene expression patterns associated with adipogenesis, osteogenesis and oxidative stress using MSCs of two different origins (bone marrow and human embryonic stem cells). The two MSCs showed similar patterns of osteogenic differentiation and reduced colony-formation ability with increasing radiation dose. The oxidative stress response was initiated at a low dose (2 Gy) of irradiation, as

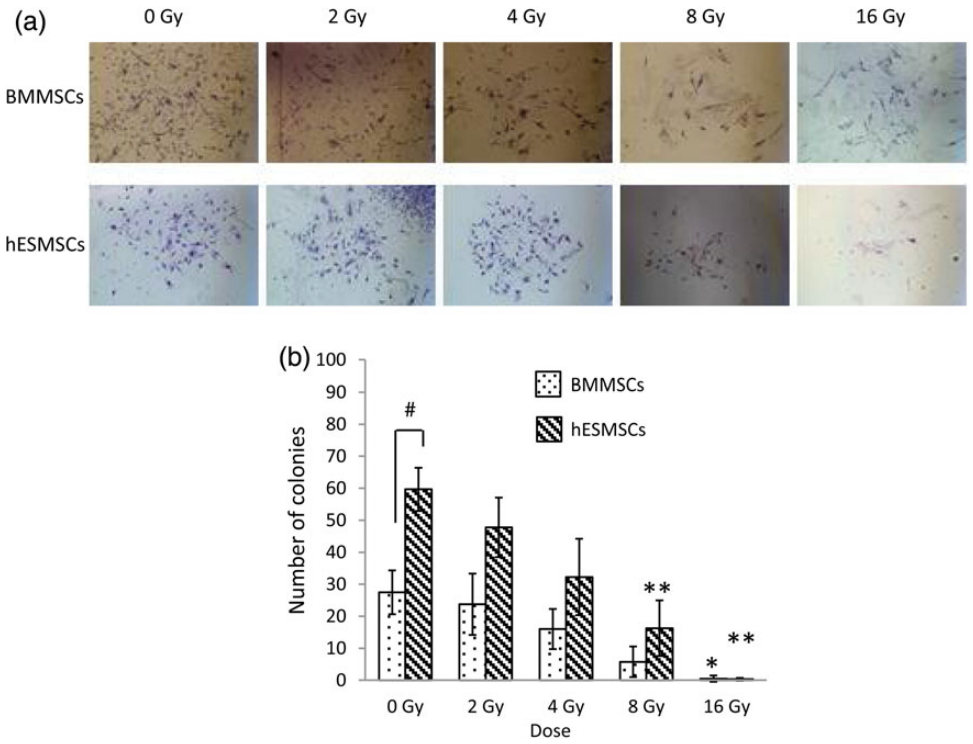

Fig. 2. Colony-forming ability of MSCs after irradiation. (**a**) Microscopic pictures of cells after Giemsa staining. (**b**) Quantitative data of colony-forming ability ($n = 4$–6). Colonies formed by MSCs was counted at 14 days after radiation. An aggregate of at least 30 cells was considered a colony. The number of colonies decreased in a dose-dependent manner. hESMSCs formed significantly higher numbers of colonies compared with BMMSCs at 0 Gy. Bars represent mean and standard error: $^{*}P < 0.05$ vs 0 Gy; $^{**}P < 0.01$ vs 0 Gy, $^{\#}P < 0.01$ vs hESMSCs.

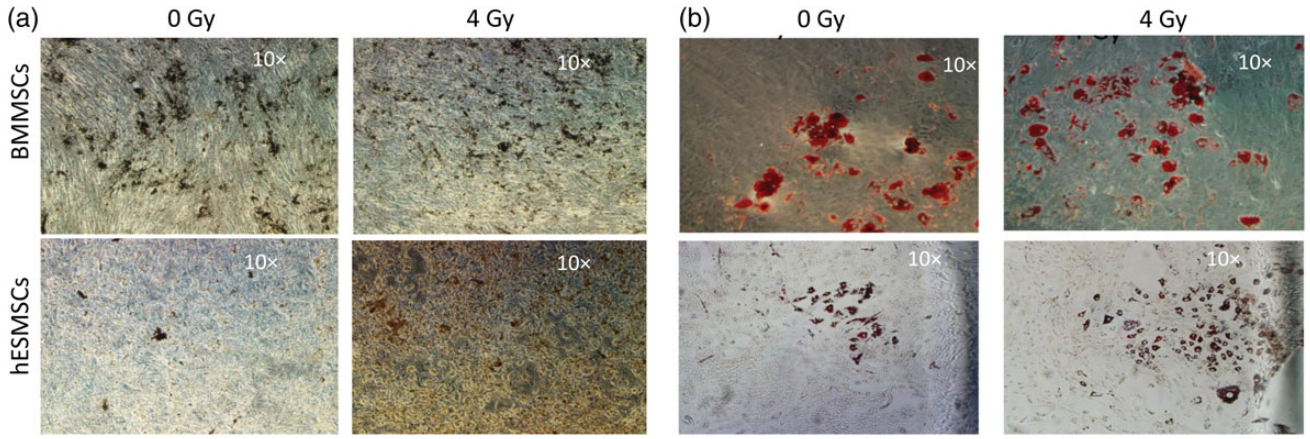

Fig. 3. Effect of irradiation on osteogenic and adipogenic differentiation in MSCs. (**a**) Osteogenic differentiation in BMMSCs and hESMSCs with von Kossa staining. (**b**) Adipogenic differentiation in BMMSCs and hESMSCs with Oil Red O staining. Osteogenic differentiation was reduced by irradiation in both MSCs. Adipogenic differentiation was increased in hESMSCs, while BMMSCs showed no change.

indicated by the higher expression of dismutase enzyme SOD1 at an early post-irradiation period (Day 1). This response remained higher as the radiation dose was increased compared with the non-irradiated groups. We found clear differences between the two types of MSCs.

Comparison of MSCs of different origins is important in order to identify a better alternative for BMMSCs. Donor BMMSCs are routinely used for transplantation to reconstitute bone marrow after therapeutic irradiation. Failure of bone marrow transplants due to graft rejection is a serious

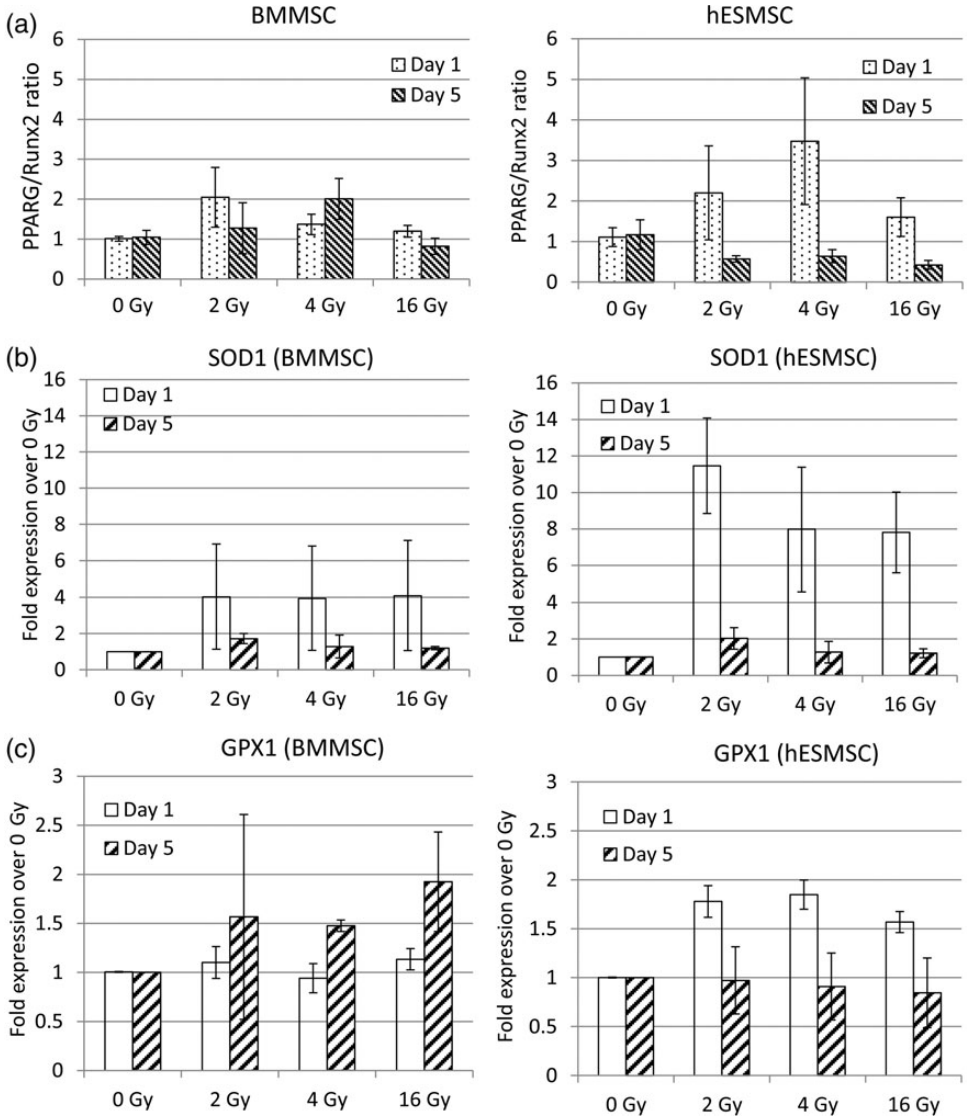

Fig. 4. Effect of irradiation on the gene expression levels of (**a**) PPARγ/RUNX2 ratio ($n = 4$–6), (**b**) SOD1 ($n = 2$–4), and (**c**) GPX1 ($n = 3$) in BMMSCs and hESMSCs 1 day or 5 days after irradiation. The ratio of PPARγ to RUNX2 expression temporarily increased in hESMSCs 1 day after irradiation. SOD1 expression was higher in the irradiated MSCs one day after radiation compared with non-irradiated MSCs. hESMSCs had higher expression of SOD1 for all doses at this time-point compared with BMMSCs. GPX1 expression did not increase much compared with 0 Gy in BMMSCs, but temporal increase was observed in hESMSCs. Each bar represents mean and standard error. No statistically significant differences were found between doses and days after irradiation.

and often fatal complication. As an alternative to this, the potential use of induced pluripotent stem cell (iPSC)-derived MSCs has generated great enthusiasm [10, 11]. iPSCs are engineered somatic cells that are pluripotent and capable of functioning as embryonically derived pluripotent cells [20]. As a transplant material, iPSC-derived MSCs are expected to have less immunogenic reaction. To support this, hESMSCs and iPSCs have been shown to have similar properties [11]. These two MSCs are developmentally more primitive cells and physiologically different from BMMSCs, which are considered adult stem cells that have lost pluripotency [21]. Understanding the radiation responses for hESMSCs is therefore important for exploring alternatives to the use of BMMSCs.

We found that the responses of hESMSCs to radiation differed greatly from those of BMMSCs. hESMSCs were highly proliferative and radiosensitive. We also found that most hESMSCs were in G2/M phase and less were in S phase compared with BMMSCs. Quitet *et al.* demonstrated that a radioresistant cell line had twice the number of cells in S-phase

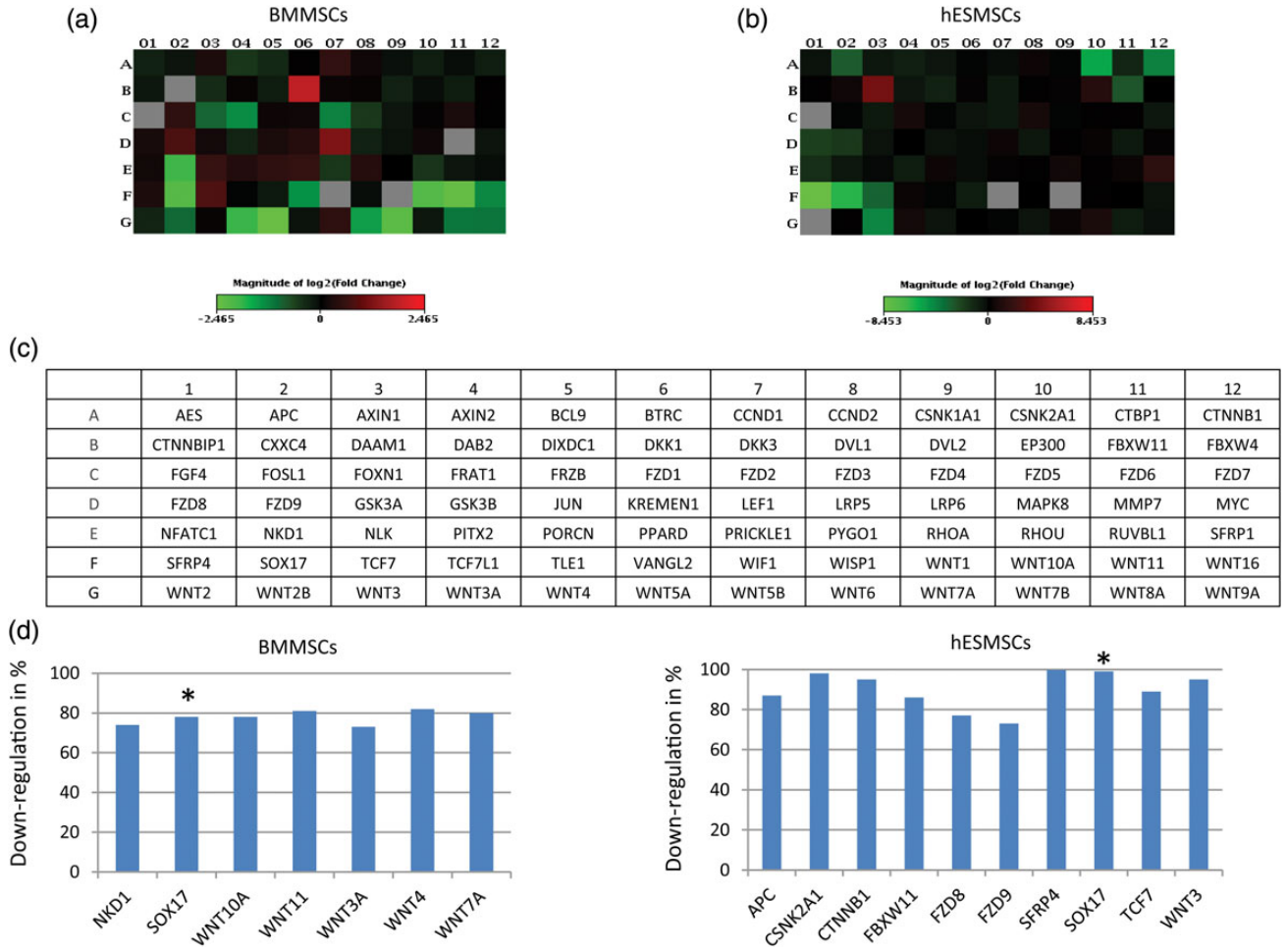

	1	2	3	4	5	6	7	8	9	10	11	12
A	AES	APC	AXIN1	AXIN2	BCL9	BTRC	CCND1	CCND2	CSNK1A1	CSNK2A1	CTBP1	CTNNB1
B	CTNNBIP1	CXXC4	DAAM1	DAB2	DIXDC1	DKK1	DKK3	DVL1	DVL2	EP300	FBXW11	FBXW4
C	FGF4	FOSL1	FOXN1	FRAT1	FRZB	FZD1	FZD2	FZD3	FZD4	FZD5	FZD6	FZD7
D	FZD8	FZD9	GSK3A	GSK3B	JUN	KREMEN1	LEF1	LRP5	LRP6	MAPK8	MMP7	MYC
E	NFATC1	NKD1	NLK	PITX2	PORCN	PPARD	PRICKLE1	PYGO1	RHOA	RHOU	RUVBL1	SFRP1
F	SFRP4	SOX17	TCF7	TCF7L1	TLE1	VANGL2	WIF1	WISP1	WNT1	WNT10A	WNT11	WNT16
G	WNT2	WNT2B	WNT3	WNT3A	WNT4	WNT5A	WNT5B	WNT6	WNT7A	WNT7B	WNT8A	WNT9A

Fig. 5. Gene expression changes in the Wnt pathway in BMMSCs and hESMSCs after irradiation of 2 Gy. (**a**) A heatmap of fold up- or downregulation in irradiated BMMSCs compared with the non-irradiated cells, (**b**) A similar heatmap for hESMSCs. (**c**) Genes in the plate. (**d**) Genes downregulated more than 70%. SOX 17 was the only gene downregulated in both BMMSCs and hESMSCs.

than the more sensitive cell line [22]. This could be a potential reason that hESMSCs have higher radiosensitivity than BMMSCs. Apoptosis induction might be another factor that influences radiosensitivity. Although Nicolay *et al.* demonstrated that the percentage of apoptotic human bone marrow MSCs was smaller than that of other fibroblasts, as assessed by the sub G1 population [13], further studies will be necessary to see the radiation effects on apoptosis in hESMSCs.

From a clinical perspective, radiation injury to bone is often manifested by increased adipogenesis and reduced osteogenesis, which makes these two mechanisms appear to be closely related. There are conflicting reports about the relationship between adipogenesis and osteogenesis [19, 23]. Similar to our findings, Li and Chan demonstrated that the osteogenic differentiation ability of MSCs is gradually lost with an increase in radiation dose [24]. Our finding of an increase in relative PPARγ expression suggests that a switch towards adipogenesis probably happens at lower doses and in early post-radiation stage.

Although the PPRAγ/RUNX2 ratio was downregulated at Day 5 after irradiation, adipogenesis was observed at Day 21 or Day 28 in both MSCs. Differentiation of MSCs to preadipocyte and ultimately to mature adipocyte is a multistep process requiring the sequential activation of several groups of transcription factors, including the C/EBP gene family and peroxisome proliferator-activated receptor [25]. Although the events of multistep processes are clearer, the exact temporal events are less known. Because PPARγ is expressed in preadipocytes, it is expected that PPARγ expression will precede the development of mature adipocyte development. Nocturnin (NOC), a circadian-regulated protein, was also reported to play a unique role in the regulation of mesenchymal stem-cell lineage allocation by modulating PPARγ activity through nuclear translocation early in the adipogenic process [26]. Furthermore, they found NOC is induced transiently in early adipogenesis, and then is robustly upregulated during the latter phases of differentiation in 3T3-L1 cells. The early upregulation of PPARγ may, therefore, have contributed to the

later adipogenic differentiation. Further studies will be required to better understand the post-radiation temporal process of adipogenic development.

We found upregulation of PPARγ and downregulation of several Wnt ligands in irradiated BMMSCs (Fig. 5). Recently, Cawthorn *et al.* demonstrated that the fate of MSCs toward adipogenesis is determined by inhibition of Wnt6, Wnt10A and Wnt10B ligands and subsequent downregulation of the Wnt-β-catenin pathway [27]. In our Wnt pathway array, we found 65% or more downregulation of Wnt6 and Wnt10A ligands (Fig. 5d). The canonical and non-canonical Wnt pathways may, therefore, be important contributors in determining the adipogenesis and osteogenesis fate of irradiated MSCs.

In conclusion, cell proliferation was faster in hESMSCs compared with BMMSCs. Consequently radiosensitivity of hESMSCs was higher than that of BMMSCs. Most hESMSCs cells stayed in G2/M phase after irradiation, but this was not found in BMMSCs. PPARγ expression was upregulated early after irradiation, along with the expression of SOD1. While downregulation of several Wnt ligands were observed in post-radiation BMMSCs cells, mostly different sets of ligands, including beta-catenin, were downregulated in post-radiation hESMSCs. However, the differentiation ability was sustained in both BMMSCs and hESMSCs after irradiation. Further studies on the Wnt-mediated fate determination of irradiated MSCs are essential for understanding of the detailed radiobiology of hESMSCs and their therapeutic utility as an alternative to BMMSCs.

SUPPLEMENTARY DATA

Supplementary data are available at the *Journal of Radiation Research* online.

ACKNOWLEDGEMENTS

The authors thank Dr Darryl Hamamoto from the Dental School for reviewing the manuscript.

FUNDING

This work was funded through an intramural start-up fund (to M.S.I.) and the National Institute of Health grant (1R01CA154491-01 to S.K.H.).

REFERENCES

1. Hui S, Verneris M, Froelich J *et al*. Multimodality image guided total marrow irradiation and verification of the dose delivered to the lung, PTV, and thoracic bone in a patient: a case study. *Technol Cancer Res Treat* 2009;**8**:23–28.
2. Wong JY, Forman S, Somlo G *et al*. Dose escalation of total marrow irradiation with concurrent chemotherapy in patients with advanced acute leukemia undergoing allogeneic hematopoietic cell transplantation. *Int J Radiat Oncol Biol Phys* 2013;**85**:148–56.
3. Carmona R, Pritz J, Bydder M *et al*. Fat composition changes in bone marrow during chemotherapy and radiation therapy. *Int J Radiat Oncol Biol Phys* 2014;**90**:155–63.
4. Rose BS, Aydogan B, Liang Y *et al*. Normal tissue complication probability modeling of acute hematologic toxicity in cervical cancer patients treated with chemoradiotherapy. *Int J Radiat Oncol Biol Phys* 2011;**79**:800–7.
5. Bolan PJ, Arentsen L, Sueblinvong T *et al*. Water–fat MRI for assessing changes in bone marrow composition due to radiation and chemotherapy in gynecologic cancer patients. *J Magn Reson Imaging* 2013;**38**:1578–84.
6. Yang X, Balakrishnan I, Torok-Storb B *et al*. Marrow stromal cell infusion rescues hematopoiesis in lethally irradiated mice despite rapid clearance after infusion. *Adv Hematol* 2012;**2012**: 142530.
7. Despars G, St-Pierre Y. Bidirectional interactions between bone metabolism and hematopoiesis. *Exp Hematol* 2011;**39**:809–16.
8. Bianco P. Minireview: the stem cell next door: skeletal and hematopoietic stem cell "niches" in bone. *Endocrinology* 2011;**152**:2957–62.
9. Barberi T, Willis LM, Socci ND *et al*. Derivation of multipotent mesenchymal precursors from human embryonic stem cells. *PLoS Med* 2005;**2**:e161.
10. Jung Y, Bauer G, Nolta JA. Concise review: induced pluripotent stem cell-derived mesenchymal stem cells: progress toward safe clinical products. *Stem Cells* 2012;**30**:42–7.
11. Lian Q, Zhang Y, Zhang J *et al*. Functional mesenchymal stem cells derived from human induced pluripotent stem cells attenuate limb ischemia in mice. *Circulation* 2010;**121**: 1113–23.
12. Katsara O, Mahaira LG, Iliopoulou EG *et al*. Effects of donor age, gender, and *in vitro* cellular aging on the phenotypic, functional, and molecular characteristics of mouse bone marrow-derived mesenchymal stem cells. *Stem Cells Dev* 2011;**20**:1549–61.
13. Nicolay NH, Sommer E, Lopez R *et al*. Mesenchymal stem cells retain their defining stem cell characteristics after exposure to ionizing radiation. *Int J Radiat Oncol Biol Phys* 2013;**87**:1171–8.
14. Olivier EN, Rybicki AC, Bouhassira EE. Differentiation of human embryonic stem cells into bipotent mesenchymal stem cells. *Stem Cells* 2006;**24**:1914–22.
15. Kopher RA, Penchev VR, Islam MS *et al*. Human embryonic stem cell-derived $CD34^+$ cells function as MSC progenitor cells. *Bone* 2010;**47**:718–28.
16. Islam MS, Ni Z, Kaufman DS. Use of human embryonic stem cells to understand hematopoiesis and hematopoietic stem cell niche. *Curr Stem Cell Res Ther* 2010;**5**:245–50.
17. Livak KJ, Schmittgen TD. Analysis of relative gene expression data using real-time quantitative PCR and the $2^{-\Delta\Delta CT}$ method. *Methods* 2001;**25**:402–8.
18. Sethe S, Scutt A, Stolzing A. Aging of mesenchymal stem cells. *Ageing Res Rev* 2006;**5**:91–116.
19. Takada I, Kouzmenko AP, Kato S. Wnt and PPARγ signaling in osteoblastogenesis and adipogenesis. *Nat Rev Rheumatol* 2009;**5**:442–7.

20. Takahashi K, Yamanaka S. Induction of pluripotent stem cells from mouse embryonic and adult fibroblast cultures by defined factors. *Cell* 2006;**126**:663–76.
21. Roura S, Farre J, Soler-Botija C *et al*. Effect of aging on the pluripotential capacity of human $CD105^{+}$ mesenchymal stem cells. *Eur J Heart Fail* 2006;**8**:555–63.
22. Quiet CA, Weichselbaum RR, Grdina DJ. Variation in radiation sensitivity during the cell cycle of two human squamous cell carcinomas. *Int J Radiat Oncol Biol Phys* 1991;**20**:733–8.
23. Yu WH, Li FG, Chen XY *et al*. PPARgamma suppression inhibits adipogenesis but does not promote osteogenesis of human mesenchymal stem cells. *Int J Biochem Cell Biol* 2012;**44**: 377–84.
24. Li J, Kwong D, Chan G. The effects of various irradiation doses on the growth and differentiation of marrow-derived human mesenchymal stromal cells. *Pediatr Transplant* 2007; **11**:379–87.
25. Rosen ED, Walkey CJ, Puigserver P *et al*. Transcriptional regulation of adipogenesis. *Genes Dev* 2000;**14**:1293–307.
26. Kawai M, Green CB, Lecka-Czernik B *et al*. A circadian-regulated gene, *Nocturnin*, promotes adipogenesis by stimulating PPAR-γ nuclear translocation. *Proc Natl Acad Sci U S A* 2010;**107**:10508–13.
27. Cawthorn WP, Bree AJ, Yao Y *et al*. Wnt6, Wnt10a and Wnt10b inhibit adipogenesis and stimulate osteoblastogenesis through a beta-catenin-dependent mechanism. *Bone* 2012;**50**:477–89.